ELSEVIER

Journal of Magnetism and Magnetic Materials 184 (1998) 319–329

journal of magnetism and magnetic materials

Low-temperature magnetic properties of Al–Pd–Mn–B quasicrystalline alloys

Dong-Liang Peng[a,*], Kenji Sumiyama[a], Kenji Suzuki[a], Akihisa Inoue[a], Yoshihiko Yokoyama[b], Kenzo Fukaura[b], Hisakichi Sunada[b]

[a] *Institute for Materials Research, Tohoku University, Katahira Sendai City, Miyagi 980-77, Japan*
[b] *Faculty of Engineering, Himeji Institute of Technology, Shosha Himeji City, Hyougo 671-22, Japan*

Received 19 September 1997; received in revised form 2 December 1997

Abstract

Low-temperature magnetic properties of the $Al_{70-x}Pd_{15}Mn_{15}B_x$ icosahedral alloys ($0 \leqslant x \leqslant 6$) were measured by a superconducting quantum interference device (SQUID). The alloy with $x = 0$ is a simple spin glass: the thermoremanent magnetization, $M_R(t)$, is characterized by a stretched exponential: $M_R(t) = M_1 + M_0 \exp[-(t/\tau)^{\beta}]$. The alloy with $x = 1$ is a cluster glass: $M_R(t)$ is also in the stretched exponential form, while the alloy with $x = 1.5$ is superparamagnetic. In alloys with $x = 1$ and 1.5, there is a very small amount of a ferromagnetic component. The alloys with $2.5 \leqslant x \leqslant 6$ are composed of a ferromagnetic component and a superparamagnetic and/or Curie–Weiss paramagnetic one. Therefore, the addition of B significantly changes the magnetic state of the Al–Pd–Mn alloys, owing to the formation and growth of magnetic Mn clusters.

PACS: 75.50. – y; 75.50.Cc; 75.60.Ej

Keywords: Icosahedral alloy; Ferromagnetism; Spin glass; Cluster glass; Superparamagnetism

1. Introduction

Development of stable quasicrystals have accelerated their structural study including the determination of atomic arrangements for various types of icosahedral and decagonal phases. Intrinsic physical properties have been observed in these stable quasicrystals: high electrical resistivity [1], pseudo-gaps at a Fermi energy level [2], high hardness [3] and a high Young's modulus [4]. Their magnetic properties are also having large attraction because any distinct spontaneous magnetization is unexpected and spin-glass-like [5–7] and/or inhomogeneous ferromagnetic phenomena [8] are desirable in the unique structures loosing a translational symmetry. However, it has been reported [9] that an icosahedral $Al_{40}Cu_{10}Mn_{25}Ge_{25}$ alloy prepared by rapid solidification has a rather large coercivity at room temperature. Icosahedral Al–Mn–Si alloys have been reported to exhibit ferromagnetic properties at low-temperatures below 100 K [10], even though the magnetization

* Corresponding author.

0304-8853/98/$19.00
PII S0304-8853(97)01161-X

values are very small even at low temperatures in spite of their high Curie temperatures.

Recently, we have studied magnetic properties of quasicrystal Al–Pd–Mn–B [11], Al–Cu–Mn–B [11], Mn–Al–Ge–B–Fe [12] and Al–Mn–Ge–B [13] systems. An excess Mn concentration usually makes the icosahedral structure unstable: a decrease in the average outer electron concentration (e/a) from an optimum value of $e/a = 1.75$ and the strain field (phason strain) due to the atomic size difference between Mn and other constituent elements leads to the transformation from quasicrystal to various types of approximate crystalline phases. In order to maintain the quasicrystal structure in a higher Mn concentration range, we chose B as an additional element, which relaxes the strain field around an excess Mn element. We found Al–Pd–Mn–B [11] icosahedral quasicrystal alloys have high magnetizations and high Curie temperatures. The magnetization value increases drastically with the increase of B content [14]. The relation between magnetization value and the strain field implies that the formation of magnetic ordering is caused by imperfection of quasicrystallinity such as large amount of phason strain fields.

In this paper, we describe magnetic characteristics of super-cooled Al–Pd–Mn–B alloys. We propose the magnetic phase diagram of the Al–Pd–Mn–B alloys including spin glass, cluster glass, super-paramagnetism, Curie–Weiss paramagnetism and ferromagnetism.

2. Experimental

Preparation methods of Al–Pd–Mn–B quaternary alloy samples were described elsewhere [14]. The alloy compositions of constituent phases were determined by chemical analyses and energy-dispersive X-ray analyses using a scanning electron microscope. The magnetic properties such as magnetization, susceptibility, relaxation of the thermoremanent magnetization (TRM) were measured using a superconducting quantum interference device (SQUID) operating in the temperature range $2 \leqslant T \leqslant 300$ K, and magnetic field range $0 \leqslant H \leqslant 50$ kOe.

3. Results

3.1. Field dependence of magnetization

Fig. 1 shows the magnetization (M–H) curves at (a) 5 K and (b) 100 K for $Al_{70-x}Pd_{15}Mn_{15}B_x$ alloys having a quasicrystalline structure. At $T = 5$ K (Fig. 1a), M increases nonlinearly for all of these alloys. For the alloys with $x \geqslant 2.5$, M increases rapidly at $H < 5$ kOe. At $T = 100$ K (Fig. 1b), the change in M as a function of H for the alloys with $x \geqslant 2.5$ is similar to that for $T = 5$ K, while the ones for the alloys with $x \leqslant 1.5$ increases slowly and the nonlinear behavior is not marked in this magnetization scale. These results indicate that the Al–Pd–Mn–B alloys with $x \geqslant 2.5$ are ferromagnetic, while those with $x \leqslant 1.5$ are paramagnetic. In

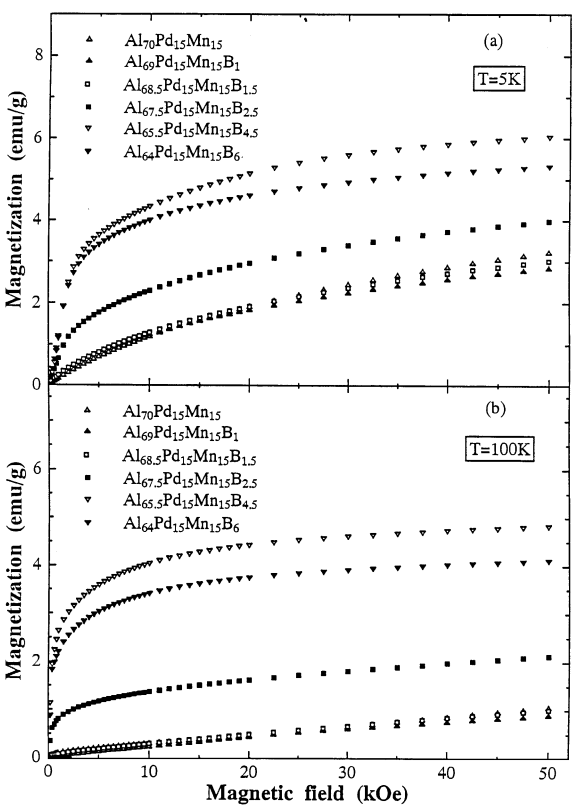

Fig. 1. Magnetization curves of the $Al_{70-x}Pd_{15}Mn_{15}B_x$ alloys with different B content at (a) 5 K and (b) 100 K.

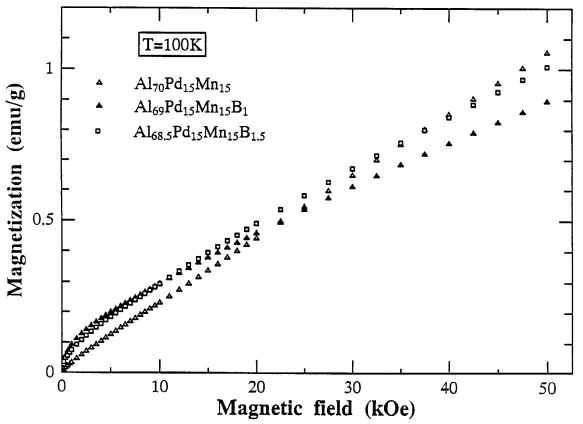

Fig. 2. Comparison of magnetization curves (at a smaller scale) of the $Al_{70-x}Pd_{15}Mn_{15}B_x$ alloys with $x = 0$, 1 and 1.5 at 100 K.

order to see more clearly the magnetization curves for the alloys with $x \leqslant 1.5$, we display the magnetization curves at $T = 100$ K in Fig. 2 with an expanded scale. As can be seen in the figure, the magnetization curve for the alloy with $x = 0$ is almost linear up to 5 T, indicating a simple paramagnetism at $T = 100$ K. But those with $x = 1$ and 1.5 are evidently nonlinear: the magnetization increases rapidly with increasing magnetic field in a low-field range ($H < 3$ kOe) and then slowly increases in a high-field range. This behavior suggests existence of small amount of ferromagnetic clusters. According to the results in Section 3.2, the $Al_{70}Pd_{15}Mn_{15}$ alloy is a spin glass (SG), while the $Al_{70-x}Pd_{15}Mn_{15}B_x$ alloys with $x = 1$ and 1.5 are cluster glass (CG) and/or superparamagnetic.

In order to obtain more information on magnetic behaviors, we show the magnetization curves for the $Al_{70}Pd_{15}Mn_{15}$ alloy having a SG feature (a), the $Al_{68.5}Pd_{15}Mn_{15}B_{1.5}$ alloy having a CG and/or superparamagnetic feature (b), and the $Al_{65.5}Pd_{15}Mn_{15}B_{4.5}$ alloy having a ferromagnetism (c) at different temperatures (Fig. 3). For the $Al_{70}Pd_{15}Mn_{15}$ alloy, the magnetization curves are almost linear at $T \geqslant 50$ K, while for the $Al_{68.5}Pd_{15}Mn_{15}B_{1.5}$ alloy, the magnetization rapidly increases with increasing magnetic field in a low-field range at all temperatures and the magnetization curves show upper convex. For the $Al_{65.5}Pd_{15}Mn_{15}B_{4.5}$ alloy (Fig. 3c), the magnetization curves clearly show a ferromagnetic behavior at all temperatures but do not completely saturate under a magnetic field of 50 kOe even at 5 K. In addition, it is worth noting that, in a low magnetic field range, the magnetization increases more rapidly at high temperature than at low temperature with increase of the magnetic field. This suggests that the icosahedral Al–Pd–Mn–B quasicrystals have a strong anisotropy.

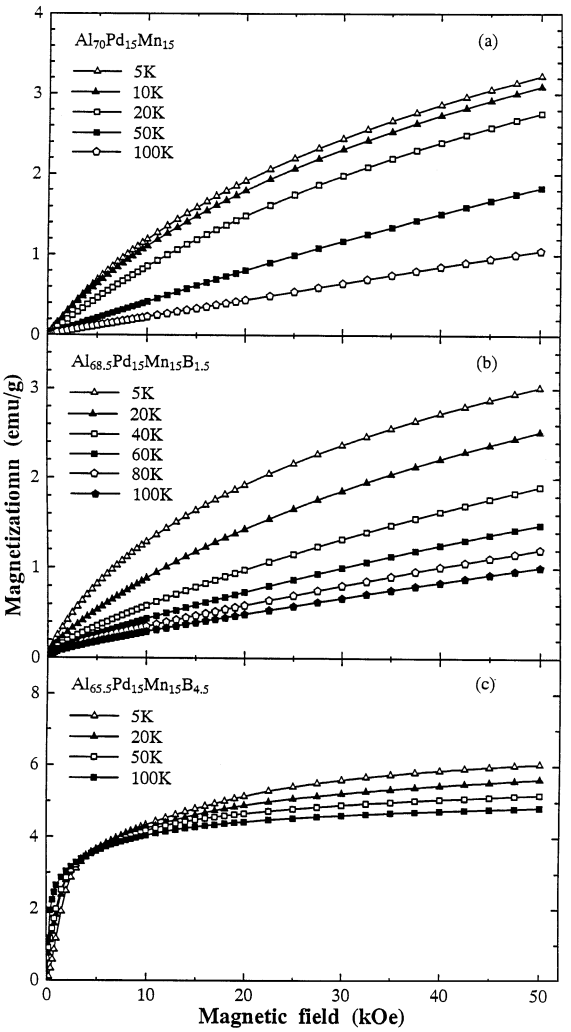

Fig. 3. Magnetization curves for the $Al_{70}Pd_{15}Mn_{15}$ alloy (a), the $Al_{68.5}Pd_{15}Mn_{15}B_{1.5}$ alloy (b), and the $Al_{65.5}Pd_{15}Mn_{15}B_{4.5}$ alloy (c) at different temperatures.

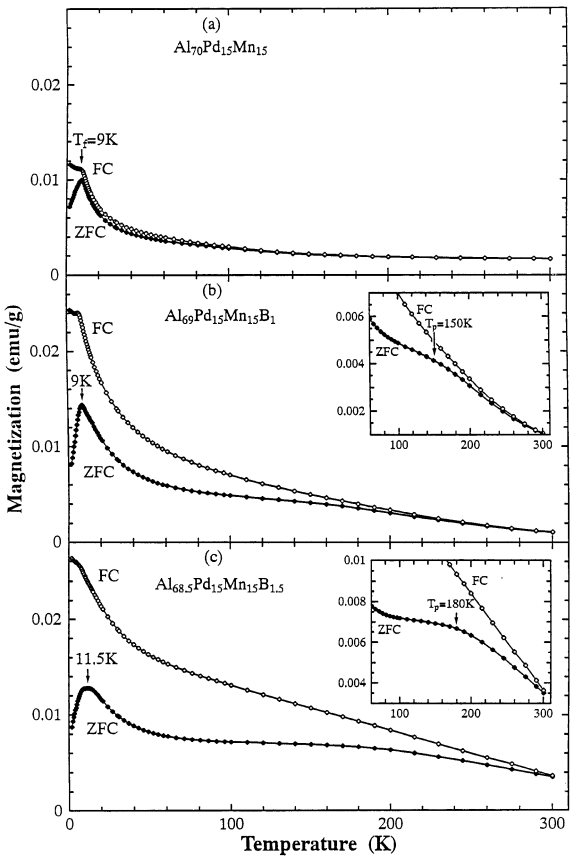

Fig. 4. Temperature dependence of magnetizations, both M_{ZFC} and M_{FC}, for the $Al_{70-x}Pd_{15}Mn_{15}B_x$ alloys with B contents of $0 \leqslant x \leqslant 1.5$.

3.2. Temperature dependence of magnetization

Fig. 4 shows the thermomagnetic curves, M_{ZFC}–T and M_{FC}–T, for the $Al_{70-x}Pd_{15}Mn_{15}B_x$ alloys with $0 \leqslant x \leqslant 1.5$. For the zero-field-cooled (ZFC) measurement, the sample was cooled in the absence of an external magnetic field from $T = 300$ to 2 K. Then H (=50 Oe) was applied and the magnetization was measured as a function of increasing temperature. For the field-cooled (FC) measurement, the sample was cooled in the presence of $H = 50$ Oe from $T = 300$ to 2 K, and then the magnetization was measured as a function of increasing temperature under this field. As seen from Fig. 4, for the $Al_{70}Pd_{15}Mn_{15}$ alloy (namely $x = 0$), a distinct magnetic cooling effect is observed at low temperature: that is, the heating and cooling curves do not coincide with each other, showing SG behavior. The freezing temperature is $T_f = 9$ K under the magnetic field of 50 Oe. For $x = 1$ (Fig. 4b) or 1.5 (Fig. 4c), a distinct cusp is also observed in the low-temperature range, and a clear difference between ZFC and FC magnetization is observed up to 300 K (see inset in Fig. 4b and c) and increases with increasing B content, while the difference between M_{ZFC} and M_{FC} is small above T_f and almost negligible above 100 K for the $Al_{70}Pd_{15}Mn_{15}$ alloy. In addition, for the alloy with $x = 1.5$, the cusp is broadened and slightly shifts to the high temperature side. This behavior seems to be related to superparamagnetism. On the other hand, as shown in the insets, the ZFC magnetization for the alloys with $x = 1$ and 1.5 exhibits a rapid decrease at higher temperature range with increasing temperature, probably due to paramagnetic transition of small amount of the local ferromagnetic Mn clusters. These results suggest that the CG, superparamagnetic and ferromagnetic phases may coexist in the $Al_{70-x}Pd_{15}Mn_{15}B_x$ $(0 < x \leqslant 1.5)$. Moreover, the increase of T_p (starting temperature of the rapid decrease of the magnetization) indicates that the strength of the exchange interaction in the local ferromagnetic Mn clusters increases with increasing B content.

Fig. 5 shows the temperature dependence of magnetization, both M_{ZFC} and M_{FC}, for the $Al_{70-x}Pd_{15}Mn_{15}B_x$ alloys with $2.5 \leqslant x \leqslant 6$. The magnetic field for the measurement is 50 Oe. These three alloys indicate almost same characteristics: the M_{ZFC} increases monotonically with increasing temperature up to 300 K and the M_{FC} decreases slowly, and the temperature dependence of M_{ZFC} and M_{FC} clearly shows the irreversibility of the magnetization. This behavior is evidently different from that for the alloys with $x \leqslant 1.5$ (Fig. 4) and is the same to that for a ferromagnetic (FM) phase with a large anisotropy energy. In order to further determine the field dependence of the irreversibility relating to the anisotropy of the FM phase in the icosahedral Al–Pd–Mn–B quasicrystals, we measured the temperature dependence of the ZFC and FC magnetizations for the $Al_{65.5}Pd_{15}Mn_{15}B_{4.5}$ alloy under different fields (Fig. 6). It is found that

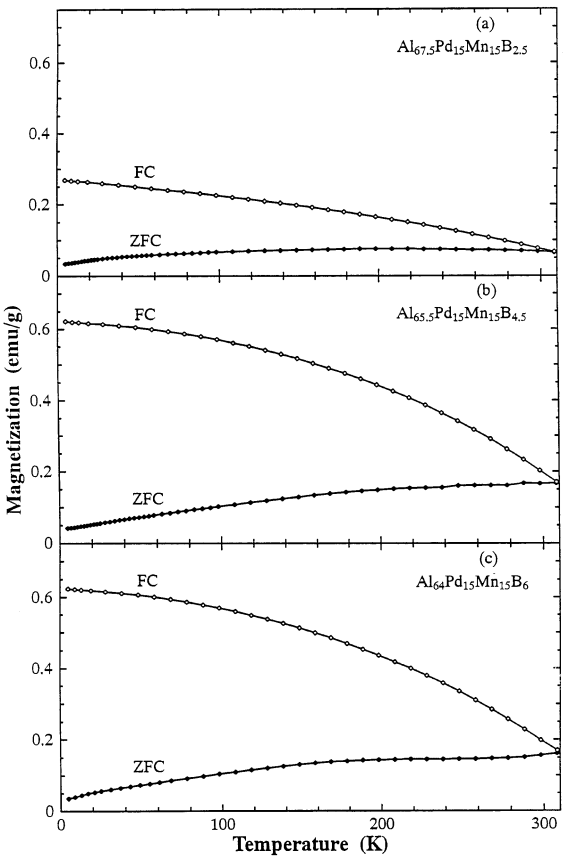

Fig. 5. Temperature dependence of magnetizations, both M_{ZFC} and M_{FC}, for the $Al_{70-x}Pd_{15}Mn_{15}B_x$ alloys with B contents of $2.5 \leqslant x \leqslant 6$.

temperatures T_{max} (corresponding to the maximum in M_{ZFC}) and T_{irr} (corresponding to starting temperature of irreversibility) below T_c decrease with the increase in the external field. Moreover, the irreversibility of magnetization persists at low temperatures even under high fields such as 10 kOe. These results confirm that there is large magnetic anisotropy in the ferromagnetic Al–Pd–Mn–B quasicrystal alloys. In addition, it is interesting that at higher fields M_{FC} rapidly increases with decreasing temperature below about 30 K. This behavior is different from the simple ferromagnetic matters, indicating that superparamagnetic or superferromagnetic phases coexists in these alloys.

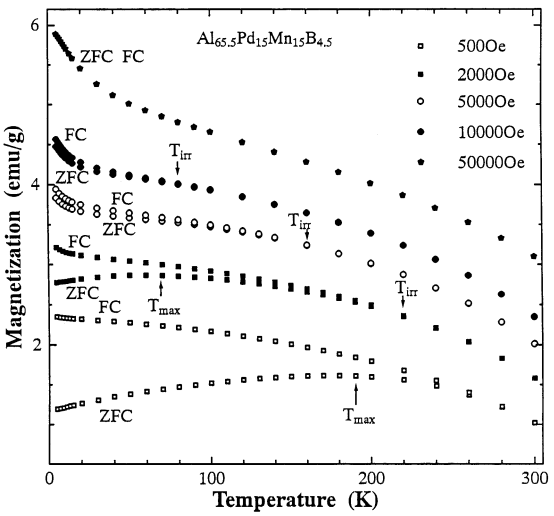

Fig. 6. Temperature dependence of the ZFC and FC magnetizations for the $Al_{65.5}Pd_{15}Mn_{15}B_{4.5}$ alloy under different magnetic fields.

4. Discussion

4.1. The $Al_{70}Pd_{15}Mn_{15}$ alloy

As shown in Section 3, the $Al_{70}Pd_{15}Mn_{15}$ alloy displays a paramagnetic to SG transition with a freezing temperature of about 9 K with cooling from room temperature to 2 K. With regard to the SG behavior in the quasicrystals, there have been reports for other series of alloys such as Al–Mn [15,16] and Al–Si–Mn [17], whose SG character can be related to the amount of the magnetic Mn atom. Because of the small amount of Mn atoms in the quasicrystals, the Mn atoms are isolated, hardly being found as the first nearest-neighboring pairs. Therefore, a long-range indirect-exchange interaction such as RKKY interaction between magnetic Mn atoms will play an important role on the SG behavior in the quasicrystals. This is also similar to magnetically dilute SG alloys such as CuMn and AuFe. So far, however, detailed investigation on the SG behavior in the quasicrystals has not been reported yet. In the following, we give some analyses on the SG behavior in the $Al_{70}Pd_{15}Mn_{15}$ alloy.

It is well known that important features of spin-glass systems are hysteresis or irreversibility after

magnetic cooling (FC) in the DC susceptibility curve as shown in Fig. 4a, and sensitivity of the cusp temperature in AC or DC susceptibility curves (ZFC) against the external magnetic field. The effect of the magnetic field on the spin-glass transition temperature has been studied extensively. Theoretically, the Sherrington–Kirkpatrick (SK) model has been studied as a mean-field theory for Ising spin glasses, where the exchange interactions are assumed to be random variables following the Gaussian distribution with a mean value J_0 and a standard deviation ΔJ [18]. In this model, de Almeida and Thouless (AT) have found that the spin-glass transition exists in finite fields [19]. In the magnetic field (H) versus temperature (T) plane, the phase boundary between the paramagnetic phase and the SG phase is called an AT line. The AT line $T_{AT}(H)$ is given approximately as a function of H by the following equation [19]:

$$H = A[1 - T_{AT}(H)/T_{AT}(0)]^{3/2}, \quad (1)$$

where the coefficient A is a function of the parameter $J_0/\Delta J$. Experimentally, $T_{SG}(H)$, defined by the onset of strong irreversibility in the temperature variation of magnetizations, is expressed by [20]

$$H = A_{exp}[1 - T_{SG}(H)/T_{SG}(0)]^{\alpha}. \quad (2)$$

The exponent α in Eq. (2) obtained from those experiments are close to the theoretical value, $\frac{3}{2}$. This result indicates that the AT line exists in SG systems. In Fig. 7, the M/H versus T curves (ZFC) under different external DC magnetic fields show a cusp-like maximum at low fields. Under $H =$ 2 Oe, the maximum is observed at 9.5 K. It shifts to 2.5 K under $H = 10$ kOe and disappears when $H > 10$ kOe.

According to the irreversibility of the ZFC and FC magnetizations under the field of 50 Oe (Fig. 4a), we roughly define the SG transition temperature $T_{SG}(H)$ as the temperature corresponding to the cusp. Using the data in Fig. 7, the magnetic field dependence of $T_{SG}(H)$ (namely magnetic phase diagram) is established in Fig. 8. We analyzed the field dependence of $T_{SG}(H)$ by using Eq. (2). In Eq. (2), $T_{SG}(0)$ is a transition temperature in zero field. As shown in the inset of Fig. 8, $T_{SG}(H)$ keeps a constant value of 9.5 K in $H < 50$ Oe. Therefore, we put $T_{SG}(0) = 9.5$ K. The solid line is the result of fitting to Eq. (2). We obtained $\alpha = 1.52$ and $A_{exp} = 1.5 \times 10^4$ Oe. Our value of α is in good agreement with the value of $\frac{3}{2}$ predicted by the theory of the AT line. This result indicates that the AT line also exists for the $Al_{70}Pd_{15}Mn_{15}$ quasicrystal SG system.

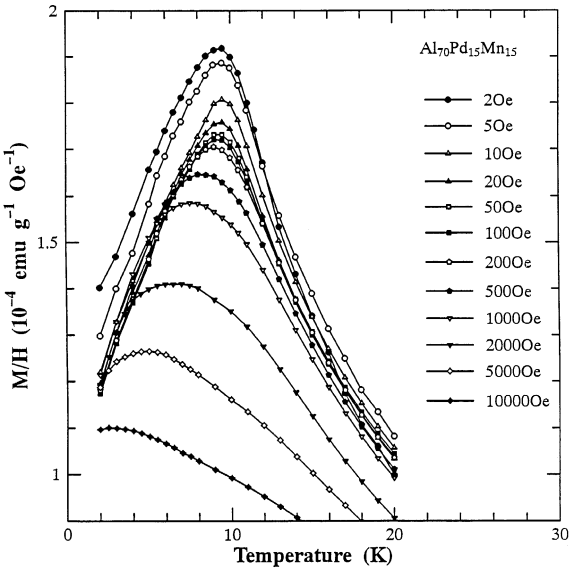

Fig. 7. M/H versus T curves (ZFC) for the $Al_{70}Pd_{15}Mn_{15}$ alloy under different external DC magnetic fields.

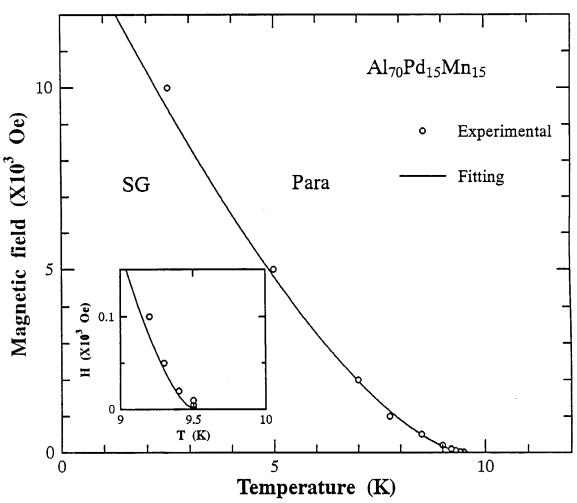

Fig. 8. Field dependence of the spin-glass transition temperature $T_{SG}(H)$ for the $Al_{70}Pd_{15}Mn_{15}$ alloy. In the inset, field dependence of $T_{SG}(H)$ in the vicinity of $H = 0$ is given at a large scale. The solid line is the result of fitting to Eq. (2).

The two most essential ingredients of a SG are frustration and quenched disorder which manifest themselves in history-dependent phenomena and eventually lead to a nonequilibrium behavior below T_f. To study the dynamical magnetic behavior in the $Al_{70}Pd_{15}Mn_{15}$ quasicrystal SG alloy, we also measured the long time decay of the field-cooled thermoremanent magnetization (TRM) around the SG transition temperature. The field-cooled TRM relaxation measurements were performed using the following procedure. We applied a small magnetic field (50 Oe) at a temperature which is 20 K higher than the SG transition temperature ($T_f = 9$ K), cooled the system to a temperature T_m which is lower than or near T_f. This FC system will be a nonequilibrium state. After waiting for 180 s the magnetic field is removed for the system to relax towards the equilibrium state and then the TRM is measured as a function of time (up to 11 500 s).

In the canonical spin glass systems such as CuMn and AgMn [21–23], TRM is represented by a stretched exponential form, as follows:

$$M(t) = M_1 + M_0 \exp[-(t/\tau)^{\beta}], \quad (3)$$

where the fitting parameters M_1, M_0, τ and β depend only on the temperature. M_1 is the value of the residual magentization, namely $M(\infty)$. $M_1 + M_0$ is the initial magnetization, written as σ_0. τ represents a characteristic relaxation time. The exponent β is $0 < \beta < 1$, differing from that ($\beta = 1$) of the conventional Debye exponential form. We found that the $Al_{70}Pd_{15}Mn_{15}$ quasicrystal SG system also satisfies such a representation of TRM, as follows.

Fig. 9 shows the variation of TRM, $M(t)$, as a function of time at different temperatures ($T_m =$ 5, 8, 12, 16, and 20 K) for constant wait time (180 s) for the $Al_{70}Pd_{15}Mn_{15}$ quasicrystal SG system. From the best fitting to Eq. (3), we found that the exponent β is almost temperature-independent, having a value of $\beta = 0.55$. This indicates that the SG $Al_{70}Pd_{15}Mn_{15}$ alloy has a very slow relaxation of TRM. The temperature dependence of the fitting parameters is shown in Fig. 10. τ, M_1 and σ_0 rapidly decrease with the increase of temperature up to 12 K ($> T_f = 9$ K) and then slowly decrease. Clearly, the variation of these parameters with the

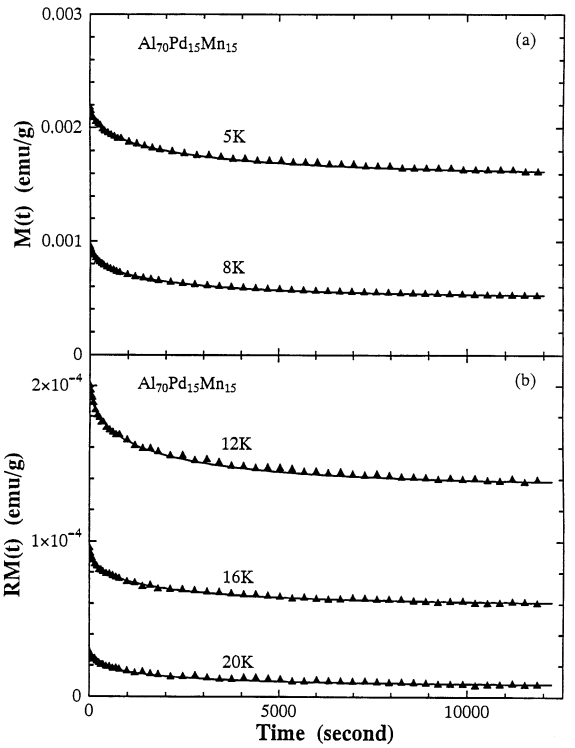

Fig. 9. TRM, $M(t)$, as a function of time in the SG ($Al_{70}Pd_{15}Mn_{15}$ alloy) for different temperatures: (a) $T_m = 5$ and 8 K and (b) 12, 16 and 20 K. Solid lines are the best fits of the data to Eq. (3).

temperature suggests that the SG state is dominant at $T < 10$ K, while the paramagnetic state becomes dominant at $T > 10$ K, leading to a small difference between σ_0 and M_1.

In order to get more information on the relaxation process, we analyze the temperature dependence of the characteristic relaxation time τ. The relaxation time for the reversal of the direction of magnetization of small, noninteracting single-domain magnetic particles can be described by an Arrhenius-type equation [24]

$$\tau = \tau_0 \exp[\Delta E_a/kT], \quad (4)$$

where k is Boltzmann's constant, T is the temperature and ΔE_a is an activation energy. As shown in the inset of Fig. 10, the Arrhenius law is found to be satisfied with $\tau_0 = 963$ s and $\Delta E_a/k = 3.62$ K over the whole temperature range investigated. This indicates that the activation energy is independent of

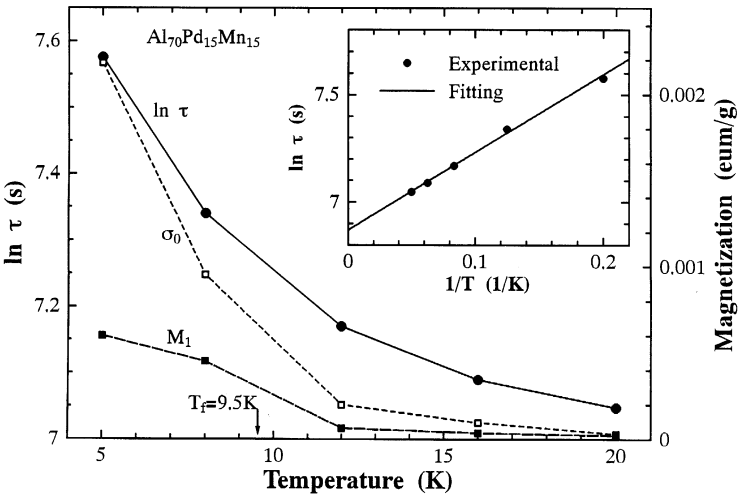

Fig. 10. Temperature variation of the characteristic relaxation time, τ, (semi-ln), initial magnetization, σ_0, and residual magnetization, M_1, in the SG ($Al_{70}Pd_{15}Mn_{15}$ alloy). The inset presents an Arrhenius plot of ln τ versus $1/T$.

the temperature, being related to the temperature-independent β exponent of the stretched exponential.

4.2. The $Al_{70-x}Pd_{15}Mn_{15}B_x$ alloy with $x = 1$ and 1.5

Because the alloys with $x = 1$ and 1.5 lie in the transition region between SG and ferromagnetism, their magnetic properties are more complicated. It is possible that several magnetic phases coexist in these alloys, where their occupation ratio depends on x. As shown in Section 3, the thermal hysteresis (see Fig. 4b and c) indicates that the alloys are CG and/or superparamagnetic. Namely, the magnetic moments of the Mn clusters are frozen below a critical temperature (T_f), and randomly oriented due to the coexistence of ferromagnetic and antiferromagnetic interactions between Mn clusters (namely a short-range RKKY-like interaction) and/or due to the magnetic anisotropy of Mn clusters without any interaction between them. As shown in Fig. 2 and in inset of Fig. 4b and c, a ferromagnetic behavior appears at the same time in these two alloys. It is also worth noting that in the $Al_{70-x}Pd_{15}Mn_{15}B_x$ icosahedral alloys, the concentration of the magnetic Mn atoms does not change and the formation of magnetic Mn clusters is only due to addition of B element whereas in numerous SG (or CG) alloys (e.g. CuMn and AuFe), the increase in magnetic impurities results in the formation of magnetic clusters. This implies that the increase of distance between Mn clusters leads to their weaker or no magnetic interaction. In this case (namely superparamagnetism), the magnetization $M(H)$ for the alloys above the freezing temperature can be written as

$$M(H, T) = M_s[\coth(\mu H/kT) - kT/\mu H] = M_s L(\mu H/kT), \quad (5)$$

where $L(\mu H/kT)$ is the Langevin function for clusters with magnetic moment μ. As expected from Eq. (5), the $M(H, T)/M_s$–H/T curves at different temperatures agree with each other for the $Al_{68.5}Pd_{15}Mn_{15}B_{1.5}$ alloy (Fig. 11), where the value of M_s is obtained by extrapolating to the magnetization value for an infinite magnetic field at 5 K (see inset). Almost all experimental data lie on the same curve, however, we found that no matter what value of μ was used, the Langevin function does not give a good fit to the $M(H)/M_s$ experimental data. In Fig. 11 the fit curve (the solid line) is obtained using a cluster average value of $\mu = 23\ \mu_B$. This indicates that the alloy is not simply superparamagnetic: the cluster size and

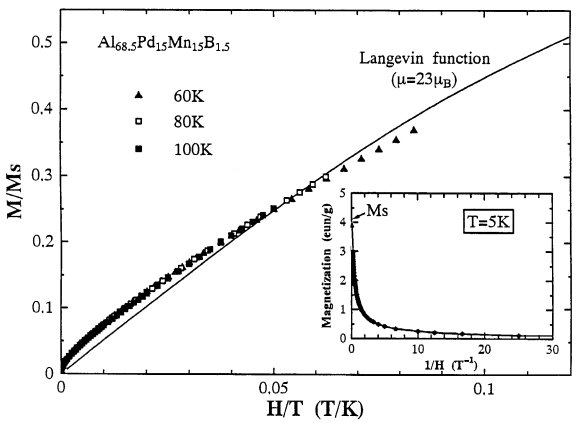

Fig. 11. $M(H, T)/M_s$–H/T curves for the $Al_{68.5}Pd_{15}Mn_{15}B_{1.5}$ alloy at several temperatures above the freezing temperature. Solid line is the result of fitting to Eq. (4) using a cluster average value of $\mu = 23\ \mu_B$.

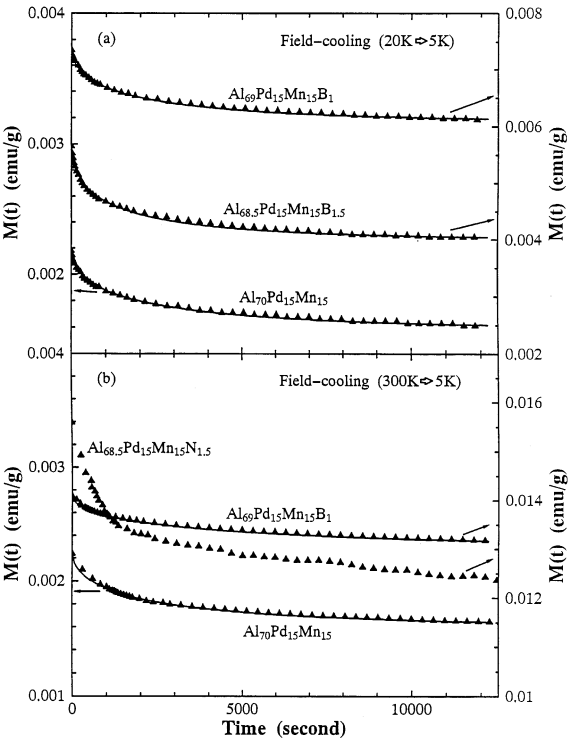

Fig. 12. Field-cooling TRM, $M(t)$, as a function of time in the $Al_{70-x}Pd_{15}Mn_{15}B_x$ alloys with $x = 0$, 1 and 1.5 at 5 K. Cooling samples under a field of 50 Oe (a) from 20 to 5 K and (b) from 300 to 5 K. Solid lines are the best fits of the data to Eq. (3).

corresponding blocking temperature are distributed [25] and a small amount of the ferromagnetic component exists.

In order to further analyze the magnetic state in the alloys with lower B content, we also measured the long time decay of the field-cooled TRM at $T = 5$ K (Fig. 12). Fig. 12a and b show the results of cooled samples under a field of 50 Oe from 20 to 5 K and from 300 to 5 K, respectively. In the case of cooling from lower temperature (20 K), the experimental data are well fitted to the Eq. (3) (the solid lines) and with same exponent: $\beta = 0.55$ for these three alloys. In the case of cooling from higher temperature (300 K), however, Eq. (3) is only suitable for the alloys with $x = 0$ and 1 but not for the alloy with $x = 1.5$. From these fits the values of M_1, σ_0 and τ are obtained (see Table 1). For the former field-cooling process, the alloys with $x = 0$ and 1 have about the same values of τ (=1950 s) which are larger than that ($\tau = 1050$ s) for the alloy with $x = 1.5$. Moreover, the values of both M_1 and σ_0 for the alloy with $x = 1.5$ are smaller than those for the alloy with $x = 1$. This result suggests that the field-cooling from the low-temperature only can make magnetic Mn atoms or smaller Mn clusters (having the RKKY interaction between them) frozen. For the latter FC process, the alloy with $x = 1.5$ has a larger σ_0 value but a smaller M_1 value than the alloy with $x = 1$, resulting from that, the field-cooling from the high temperature can make larger magnetic Mn clusters frozen (the larger σ_0 value) and also indicating that the interaction between the larger clusters is weaker or zero and thus, the magnetic relaxation occurs rapidly (the smaller M_1 value).

Therefore, the analytic results above suggest that in the $Al_{69}Pd_{15}Mn_{15}B_1$ alloy, the individual Mn atoms and the smaller magnetic Mn clusters which arise due to the addition of small amount of B element are dominant, where their magnetic moments are aligned in different directions due to the oscillation-type RKKY interaction. Therefore, this alloy mainly shows a CG behavior and has the same freezing temperature (see Fig. 4a and b) and the same relaxation form of TRM to the $Al_{70}Pd_{15}Mn_{15}$ alloy which shows a SG behavior. In the $Al_{68.5}Pd_{15}Mn_{15}B_{1.5}$ alloy, the number of

Table 1
Best-fitted parameters for Eq. (3) for field-cooling from 20 and 300 K for the alloys with $x = 0$, 1, and 1.5

Field-cooling method	B content x	τ (s)	σ_0 (10^{-3} emu/g)	M_1 (10^{-3} emu/g)
From 20 K	0	1950	2.18	1.58
	1	1950	7.36	6.06
	1.5	1050	5.65	4.01
From 300 K	0	2200	2.25	1.60
	1	4000	14.1	13.0
	1.5	/	15.6[a]	12.4[a]

[a]The parameters are obtained from experiment points but not from fitting data.

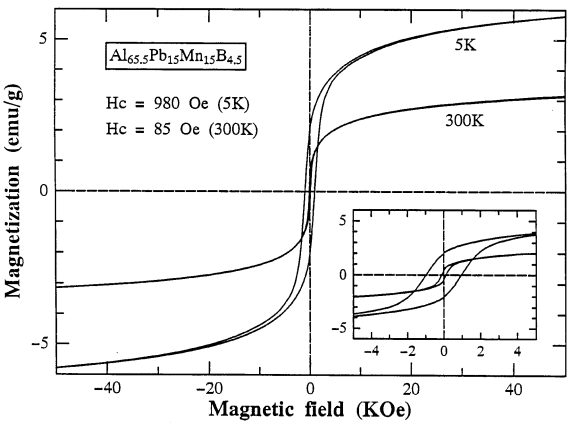

Fig. 13. The hysteresis loops of the $Al_{65.5}Pd_{15}Mn_{15}B_{4.5}$ alloy at 5 and 300 K.

the Mn clusters increases but the interaction between them is so weak that this alloy mainly shows a superparamagnetism. As shown in Fig. 4c, the broad temperature-dependent maximum in M_{ZFC} is attributable to such a magnetic feature: the various Mn clusters with different sizes and anisotropy axes are blocked at different temperatures.

4.3. The $Al_{70-x}Pd_{15}Mn_{15}B_x$ alloy with $2.5 < x \leqslant 6$

As described in Section 3, the magnetic properties of the Al–Pd–Mn–B icosahedral alloys depend strongly on the B content. The addition of B relaxes the strain field around an excess Mn element in the icosahedral atomic configuration, and simultaneously, causes an appearance of the ferromagnetism in these alloys [2]. Fig. 13 shows the hysteresis loops of the $Al_{65.5}Pd_{15}Mn_{15}B_{4.5}$ alloy. The coercivity at room temperature and 5 K is 85 and 980 Oe, respectively. The irreversibility in the high-temperature range in Fig. 6 is due to a large magnetic anisotropy and the associated large coercivity field.

Assuming that ferromagnetic and Curie–Weiss paramagnetic regions are dispersed in Pauli paramagnetic matrices of the Al–Pd–Mn–B alloys, the occupation of each magnetic component has been discussed [14]. With increasing the B content, the ferromagnetic and Curie–Weiss paramagnetic Mn clusters increase while the Pauli paramagnetic region decreases in the range of B content for $x \geqslant 3$. In this case, the large Mn clusters with a multi-domain structure are dominant, being ferromagnetic and the small Mn clusters with a single-domain structure coexist, being Curie–Weiss paramagnetic or superparamagnetic. Because the interaction between the clusters is negligible, their susceptibility is inversely proportional to T ($\chi \propto 1/T$), leading to a rapid increase in the magnetization or susceptibility with decreasing temperature below about 30 K. It should be also noted that the temperature T_{irr} at which the M_{ZFC} and M_{FC} branches deviate from each other is found to be strongly magnetic-field-dependent, indicating that the alloy has a large magnetic anisotropy.

5. Conclusions

We have measured in detail the field- and temperature-dependence of the magnetization for the $Al_{70-x}Pd_{15}Mn_{15}B_x$ icosahedral alloys with $0 \leqslant x \leqslant 6$ below room temperature. The main results are summarized as follows.

1. The $Al_{70}Pd_{15}Mn_{15}$ quasicrystalline alloy is a SG, having the freezing temperature of 9.5 K. The AT line exists in this quasicrystal SG system. The time relaxation of the TRM can be characterized by a stretched exponential form: $M(t) = M_1 + M_0 \exp[-(t/\tau)^{\beta}]$ ($\beta = 0.55$).

2. The $Al_{70-x}Pd_{15}Mn_{15}B_x$ alloy with $x = 1$ mainly shows a CG behavior and has the same stretched exponential form in the TRM as observed for $x = 0$, but the values of the characteristic relaxation time (τ), initial magnetization (σ_0) and residual magnetization (M_1) are larger than those for the $Al_{70}Pd_{15}Mn_{15}$ alloy. The $Al_{70-x}Pd_{15}Mn_{15}B_x$ alloy with $x = 1.5$ is superparamagnetic. In these two alloys, a very small amount of the ferromagnetic Mn clusters are detectable.
3. The $Al_{70-x}Pd_{15}Mn_{15}B_x$ alloys with $2.5 \leqslant x \leqslant 6$ are ferromagnetic, having strong magnetic anisotropy. But due to the coexistence of the superparamagnetic and/or Curie–Weiss paramagnetic phase in these alloys, the magnetization does not saturate even under a high field of 50 kOe and the high-field magnetization or susceptibility rapidly increases with decreasing temperature below 30 K.

Acknowledgements

The authors thank Dr. D.X. Li and Dr. T. Hihara for their helpful discussions.

References

[1] K. Kimura, H. Yamane, T. Hashimoto, S. Takeuchi, Mater. Sci. Eng. 99 (1988) 435.
[2] T. Fujiwara, T. Yokokawa, in: T. Fujiwara, T. Ogawa (Eds.), Solid-State Science 93, Quasicrystals, Springer, Berlin, 1990, p. 196.
[3] S. Takeuchi, H. Iwanaga, T. Shibuya, Jpn. J. Appl. Phys. 30 (1991) 561.
[4] Y. Yokoyama, A. Inoue, T. Masumoto, Mater. Trans. JIM 34 (1993) 135.
[5] K. Fukamichi, T. Goto, H. Komatsu, H. Wakabayashi, A.P. Tsai, A. Inoue, T. Masumoto, J. Physique C 8 (1988) 239.
[6] K. Fukamichi, T. Goto, Sci. Rep. Res. Inst. Tohoku Univ. A 34 (1989) 267.
[7] T. Goto, T. Sakakibara, K. Fukamichi, J. Phys. Soc. Japan 57 (1988) 1751.
[8] Y. Yokoyama, A. Inoue, T. Masumoto, Mater. Sci. Eng. A181/A182 (1994) 734.
[9] A.P. Tsai, A. Inoue, T. Masumoto, N. Kataoka, Jpn. J. Appl. Phys. 27 (1988) L2252.
[10] R.A. Dunlap, M.E. McHenry, V. Srinvias, D. Bahadur, R.C. O'Handley, Phys. Rev. B (1989) 4808.
[11] Y. Yokoyama, A. Inoue, T. Masumoto, Mater. Trans. JIM 33 (1992) 1012.
[12] Y. Yokoyama, A. Inoue, Mater. Trans. JIM 37 (1996) 559.
[13] Y. Yokoyama, A. Inoue, Jpn. J. Appl. Phys. 35 (1996) 3533.
[14] Y. Yokoyama, A. Inoue, H. Yamauchi, M. Kusuyama, T. Masumoto, Jpn. J. Appl. Phys. 33 (1994) 4012.
[15] K. Fukamichi, T. Masumoto, M. Oguchi, A. Inoue, T. Goto, T. Sakakibara, S. Todo, J. Phys. F 16 (1986) 1059.
[16] K. Fukamichi, T. Goto, T. Masumoto, T. Sakakibara, M. Oguchi, S. Todo, J. Phys. F 17 (1987) 743.
[17] J.J. Hauser, H.S. Chen, J.V. Waszczak, Phys. Rev. B 33 (1986) 3577.
[18] D. Sherrington, S. Kirkpatrick, Phys. Rev. Lett. 35 (1975) 1792.
[19] J.R.L. de Almeida, D.J. Thouless, J. Phys. A 11 (1978) 983.
[20] H.A. Katori, A. Ito, J. Phys. Soc. Japan 63 (1994) 3122.
[21] R.V. Chamberlin, G. Mozurkenich, R. Orbach, Phys. Rev. Lett. 52 (1984) 867.
[22] R.V. Chamberlin, J. Appl. Phys. 57 (1985) 3377.
[23] D. Chu, G.G. Kenning, R. Orbach, Phys. Rev. Lett. 72 (1994) 3270.
[24] L. Néel, Ann. Geophys. 5 (1949) 99.
[25] B.J. Hickey, M.A. Howson, S.O. Musa, G.J. Tomka, B.D. Rainford, N. Wiser, J. Magn. Magn. Mater. 147 (1995) 253.